The Importance of Secondary Cratering to Age Constraints on Planetary Surfaces

Alfred S. McEwen[1] and Edward B. Bierhaus[2]

[1]Department of Planetary Sciences, Lunar and Planetary Lab, University of Arizona, Tucson, Arizona 85721; email: mcewen@pirlmail.lpl.arizona.edu

[2]Space Systems Company, Lockheed-Martin, Denver, Colorado 80201; email: edward.b.bierhaus@lmco.com

Annu. Rev. Earth Planet. Sci. 2006. 34:535–67

First published online as a Review in Advance on January 31, 2006

The *Annual Review of Earth and Planetary Science* is online at earth.annualreviews.org

doi: 10.1146/annurev.earth.34.031405.125018

0084-6597/06/0530-0535$20.00

Key Words

impact processes, Moon, Europa, Mars, asteroids, chronology

Abstract

Small craters (less than one kilometer diameter) can be primary craters produced by impact of interplanetary debris, or they can be secondary craters produced by fallback of high-velocity ejecta blocks from much larger but infrequent primary impacts. The prevalent assumption over recent decades has been that primaries are most abundant, so most small craters are independent random events and can be used for dating. However, recent results from Europa and Mars support the early theory that distant secondaries globally dominate the number of small lunar craters; this would invalidate part of production functions that have been widely used for age dating. Crater excavation results in higher mean ejection velocities for smaller fragments, resulting in a steeper size-frequency distribution for secondary craters than is produced by the same size-frequency distribution of interplanetary debris. This review also discusses how small craters can sometimes be used to derive meaningful age constraints.

INTRODUCTION

Size-frequency distribution (SFD): the abundance of an entity (e.g., craters or rocks) as a function of the diameter of that entity

Primary crater: crater produced by impact of interplanetary debris

Secondary crater: crater produced by impact of ejecta thrown out by a primary impact on that same body

Planetocentric debris: solid material produced within a planetary system that escapes from the body of origin but remains in orbit around the planet and may impact a satellite

Crossover diameter: crater diameter below which secondaries are most abundant and above which primaries are most abundant

Analyzing the size-frequency distribution (SFD) of impact craters on the surfaces of planetary bodies beyond Earth is the fundamental technique used for relative age dating of terrains or modification processes (Shoemaker et al. 1962). The basic idea is that because crater densities increase over time owing to the random "rain" of primary impacts, absolute ages can be estimated if the cratering rate over time is estimated, as has been done for the Moon with radiometric age dating of returned samples from known locations. The SFD of craters is normally an inverse power-law function, which means that the number of craters with a certain diameter range increases markedly as diameter decreases. Relatively small craters are the most abundant, so they can be the most useful for dating young and/or small-area surfaces, but only if the statistics are dominated by primary craters.

Secondary cratering occurs on any body where primary craters form and gravitational acceleration is sufficient for ejecta blocks to fall back at a velocity that forms craters. There are environments less conducive to extensive secondary crater populations, such as bodies with thick atmospheres (e.g., Venus, Earth, and Titan) that decelerate the ejecta, or objects with insufficient surface gravity to retain much ejecta that impacts with sufficient velocity to form secondaries, or objects with high resurfacing rates that quickly erase small craters (especially Io). Thus secondary craters are abundant on objects such as the Moon, Mercury, Mars, Europa, Ganymede, and Callisto. Secondary cratering is not well understood on medium-sized bodies such as Triton, Pluto, Charon, large asteroids, and many satellites of Saturn and Uranus—mainly due to lack of data—but secondaries must form and should be widely dispersed on these objects. Escaped impact ejecta from satellites become planetocentric debris, which may eventually crater the original satellite or a different object in the system; this review does not consider this type of crater. However, we note that abundant distant secondary craters on larger bodies imply that abundant planetocentric debris will be generated by primary impacts into medium-sized satellites.

Secondary craters form from ejecta fragments generated within the gravity field of the cratered body, resulting in fields of craters that are clustered in space and time and that have a steep SFD (abundances increase rapidly towards smaller crater diameters) owing to the SFD of the fragments and an inverse size-velocity correlation of the fragments. Secondary craters cannot be used for age dating by comparison of crater spatial density because huge numbers of them form nearly simultaneously such that two surfaces of equal age may differ in small-crater densities by several orders of magnitude. However, if their provenance is known, then secondaries and rays provide useful stratigraphic markers (Shoemaker & Hackman 1962). To derive meaningful age constraints on planetary surfaces, it is essential to distinguish correctly between primary and secondary craters, at least statistically.

On many bodies, the crater SFD is steeper for craters smaller than a certain size, often ~1 km, which can be explained by an overwhelming number of secondary craters relative to primary craters and/or a change in power-law slope (or exponent) of the primary production function. Determining a terrain's crossover diameter (if it has one), below which secondaries are more abundant than primaries, is critical to

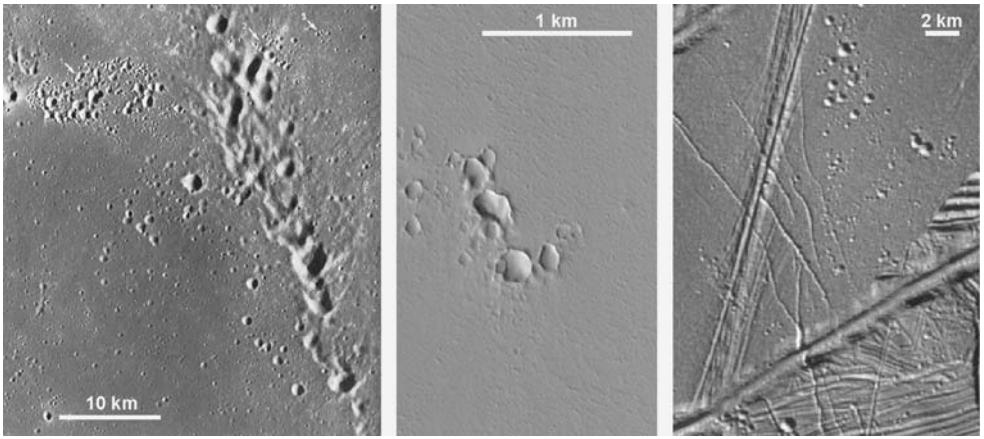

Figure 1

Secondary crater clusters. (*Left*) Image AS17-3093 from the Apollo 17 Panoramic camera showing a secondary crater chain with herringbone patterns from Copernicus (located ~350 km to the southeast). Superimposed (younger) secondary clusters may have come from Aristarchus, 580 km to the west (Masursky et al. 1978). Randomly distributed small craters in this image may be distant secondaries or small primaries. (*Middle*) A cluster of secondary craters on Mars in Amazonis Planitia, which originated from Tooting, a young 29-km diameter crater located ~100 km to the north. Mars Orbital Camera (MOC) image S05-00491, 4.5 m pixel^{-1}, available at **http://www.msss.com/mars_images/moc/publicresults/**. (*Right*) Clusters of impact craters on Europa; Galileo image E17STRSLP01, 39 m pixel^{-1}. The secondaries from Aristarchus and those on Europa are distant secondaries (>10 times the radius of the primary crater).

deriving age constraints for young terrains and for older terrains covering small areas, i.e., where only small craters are superimposed on the unit in significant numbers. Age constraints are essential to quantitative understanding of surface processes (e.g., Doran et al. 2004), and crater-density comparison is the primary method available to estimate ages for planetary surfaces other than those on Earth.

Regolith: unconsolidated (loose) material covering a planetary surface, generated by any process (impact, volcanic, fluvial, glacial, eolian, biological, etc.)

A secondary origin is obvious for the fields of small craters surrounding large primary craters, which exhibit distinctive morphologies such as shallow, irregular shapes and occurrence in chains and clusters, sometimes with distinctive herringbone patterns (e.g., Shoemaker 1962, Oberbeck & Morrison 1973) (see **Figure 1**). However, there has been a long-standing controversy about the abundances of small primaries versus distant secondaries on the Moon. Distant secondaries produced by high-velocity ejecta fragments are more circular and may be less clustered than the adjacent secondaries, and can therefore be difficult to distinguish from primaries given the finite resolution of remote imaging. Shoemaker (1965) hypothesized that there may be enormous numbers of these distant or "background" secondaries. That view fell out of favor (in most publications) by the early 1980s, but is now experiencing a revival.

Understanding secondary cratering is important to assessing regolith formation, rock distributions, and impact hazards on bodies that lack thick atmospheres, and

Hypervelocity impact: impact velocity faster than the sound speed of target material, producing a shock wave through that material

the secondary craters provide constraints on models of cratering mechanics and constitute a semicontrolled experiment on the properties of target materials. However, this review focuses on the importance of secondary cratering in constraining the ages of surface units. We begin with a tutorial on small-crater formation and characteristics, review the lunar controversy, and describe recent results from Europa and Mars. We then describe why secondaries must usually dominate the numbers of small craters, discuss the problem of determining the primary production functions for small craters, and review how small craters can sometimes be used for meaningful age constraints.

CHARACTERISTICS OF PRIMARY AND SECONDARY CRATERS

Decades of theoretical, experimental, and, most recently, numerical research have explored the physics of crater formation. Secondary craters form from ejecta launched during the excavation of a primary crater; thus understanding the processes of crater excavation is crucial to understanding the relative contribution of secondaries to crater SFD. See Melosh (1984, 1989) for more thorough descriptions of the excavation process. Briefly, crater size and morphology for both primary and secondary craters are a function of impact velocity/energy, impact angle, projectile type, and target type.

Impact Velocity/Energy

Primary craters are formed by hypervelocity impacts, meaning that the impact energy is sufficient to generate initial shock waves with velocities higher than the sound speed of the material. Average impact speeds for planet-crossing asteroids are $\sim$16 km s^{-1} on the Moon and $\sim$10 km s^{-1} on Mars (Ivanov 2001), whereas on Europa the cometary impact velocity averages $\sim$20 km s^{-1} (Zahnle et al. 1998). The impact speeds for secondaries are limited (approximately) by the escape velocity of the primary target body—approximately 5 km s^{-1} for Mars, 4.2 km s^{-1} for Mercury, 2.4 km s^{-1} for the Moon, and 2 km s^{-1} for Europa. The escape velocity is a factor of two smaller than the average primary impact velocity for Mars, but an order of magnitude smaller than the primary impact velocity for Europa. Secondary impact velocities are usually below hypervelocity speeds, but nevertheless generate stress impulses exceeding elastic limits (Melosh 1989).

Impact Angle

The average impact angle (measured from local horizontal) for a primary impact between two objects orbiting the Sun is approximately 45° (Gilbert 1893, Shoemaker 1962). Primary impact craters exhibit circular shapes at impact angles as low as 10°, at which point they become increasingly elliptical, which suggests that impact angle has a weak effect on primary-crater shape except in low-angle impacts (Gault & Wedekind 1978, Melosh 1989).

However, the material ejected during the crater formation process, i.e., the material that forms secondary craters, has a stronger dependence on the primary impact angle. Experiments show that the ejection angle of material excavated from a primary impact, and thus the impact angle of the ejected material, is a function of ejection time (Shoemaker 1962, Oberbeck 1975). The early material, ejected from a vertical impact during the contact and compression stage and with the fastest velocity, also has the highest ejection angle, perhaps 60°–70°. As excavation proceeds through spallation and the bulk excavation flow, the ejection angle decreases to approximately 45°, dropping to perhaps 30° for the late-stage ejecta that falls close to the primary crater. Other impact experiments (Anderson et al. 2003) show that a 45° primary impact enhances the velocity of downrange ejecta relative to uprange ejecta, with increasing asymmetries in the velocity distribution as primary impact angle decreases. Oblique primary impacts also change the distribution of ejection angles within the ejecta curtain, creating a lower ejection angle (<45°) for the high-velocity downrange ejecta.

Spallation: the fragmentation and ejection of the near-surface layer surrounding an impact, caused by the interaction of the impact shock wave with the surface

A single primary impact, with a typical impact angle of 45°, generates ejecta with a suite of ejection (and thus secondary impact) angles. Combined with the mass-velocity distribution, a single primary generates ejecta that reimpacts with numerous combinations of impact velocity, energy, and angles so that the secondary crater population will have a range of morphologies over a uniform target type.

Target Type

Target type has a significant influence on the excavation processes and the resulting primary crater. Strength, porosity, layering, and equations of state of the projectile and target materials all contribute to the details of ejecta production. Numerical simulations by Head et al. (2002) demonstrated that regolith dampens the production of high-velocity ejecta during an impact, and the SFD of rocks in the regolith affects the secondary crater sizes. High-porosity targets produce little ejecta in vertical impacts, as such craters likely form primarily by compaction (Holsapple et al. 2002), although Yamamoto (2002) and Yamamoto et al. (2005) found that oblique impacts into powders generate greater volumes of high-velocity ejecta. The target type not only influences ejecta formation, but also influences the response to fragment reimpact and the resulting morphologies of secondary craters.

Projectile Type

Impacts by comets and asteroids form primary craters. The densities and interior structures are well constrained for some asteroids, but still inferred for most asteroid types and comets. Melosh (1989) estimated the penetration depth at constant velocity, equivalently the origin of the impact shock wave, as $d = 2a(\rho_p/\rho_t)^{1/2}$, where a is projectile radius, ρ_p is the projectile density, and ρ_t is the target density. There may not be a standard penetration depth for a given-sized primary projectile, as there appears to be a range of densities for different asteroid types (e.g., Britt et al. 2002), and although thought to be low (less than 1 g cm^{-3}), comet densities are not well known. Recent results from the Deep Impact experiment indicate a bulk density for

comet Temple 1 of ~0.6 g cm^{-3} (A'Hearn et al. 2005). Smaller penetration depths lead to thinner spallation zones and less high-velocity ejecta; thus a cometary impact at 35 km s^{-1} produces a comparable amount of high-speed ejecta as a denser asteroidal body with the same volume impacting at 10 km s^{-1} in the simulations of Artemieva & Ivanov (2004).

Flying chunks of the target surface form secondary craters. The physical state (e.g., bulk density) of the fragments is not known, but observations of coherent blocks around smaller primary-crater rims on the Moon and Mars (Bart & Melosh 2005), as well as the presence of blocks ejected from Ries crater in Germany (Horz et al. 1983), suggest that some of the fragments are solid pieces of the target material. Thus, if the target terrain has a uniform density, then the fragments that create secondaries may all have similar penetration depths (on the order of the fragment diameter) for similarly sized solid fragments, rather than the range of values exhibited by primary projectiles. However, impacts by tight clumps of ejecta (forming single craters) are also expected to be common (Schultz & Gault 1985, Melosh 1989).

Formation Frequency and Proximity

The impacts that form primary craters occur randomly in time and space (with the exception of asymmetries on the leading versus trailing hemispheres of satellites in synchronous orbits). The impact flux is a function of the dominant projectile population and a target's proximity to that population; the asteroid belt dominates the flux in the inner Solar System (Ivanov et al. 2002), whereas comets and planetocentric debris dominate in the outer Solar System (Zahnle et al. 2003).

The rate at which secondary crater fields form is the same as for large primary impacts, i.e., secondaries appear only when a primary of sufficient size forms, but millions of secondaries may form from a single primary in an instant of geologic time. Many of these secondaries form in close proximity to one another, such that their formation affects neighboring secondaries, chiefly by interacting excavation flows and ejecta curtains (Oberbeck 1975).

Sizes and Morphologies

Primary impact craters range in size from microscopic pits caused by pieces of high-velocity dust on airless bodies to enormous basins thousands of kilometers in diameter (up to sizes above which the target body could be disrupted). Small craters have a simple bowl shape. Larger craters begin to have flat floors and perhaps terraced walls. Still-larger craters have internal features such as a central peak, peak ring, or pit, whereas giant impact basins can have roughly concentric, multiringed structures. The transitions between crater morphologies are a function of the surface gravity and material strength of the layers penetrated by the crater cavity. The smaller, bowl-shaped craters are in the strength regime, where the material strength of the target can support the topography of the crater. Larger craters transition into the gravity-dominated regime, where gravity overcomes the material strength of the surface and causes

further collapse of the crater, forming complex craters with flat floors, terraced walls, and central peaks or pits.

In contrast, secondary craters have a maximum diameter dictated by the size of their parent craters. The maximum secondary crater diameter is typically <5% of the parent primary (<0.05 D_p), which holds true for measurements on the Earth, Moon, Mars, Mercury, and Europa (Shoemaker 1965, Schultz & Singer 1980, Bierhaus et al. 2001). The maximum size may depend on the range at which secondaries appear; for secondaries within a few crater radii of their parent primary, the maximum diameter is closer to 0.05 D_p, whereas for secondaries that first appear at greater ranges from their parent primary [e.g., Zunil on Mars (McEwen et al. 2005)], the value is less, approximately 0.025 D_p. There may also be a threshold diameter for the smallest primary that produces secondaries; though the threshold diameter is not well characterized, it varies as a function of surface properties. Secondary impact velocities are restricted to less than the escape velocity of the parent body. Most secondaries (except those from basins) are small due to the steep SFD and thus form with simple-crater morphologies, but they are not necessarily circular, bowl-shaped cavities.

Secondaries within ~10 crater radii of their parent craters usually exhibit distinctive morphologies: They are elliptical in plan, tend to be shallower than primaries of a similar size, may have distinctive chevron patterns between closely spaced individual craters, and form in loops and chains (**Figure 1**). The morphology of more distant secondaries approaches that of small primaries, but often with significant clustering, although detailed morphological studies are rare because of the difficulty in identifying craters as primary or secondary as (*a*) the relevant diameters approach the resolution limits of available image data and (*b*) it can be difficult to identify the source crater for distant secondaries. To the degree that researchers have been able to identify and quantify secondary crater morphologies (mostly within the Mars data sets, see McEwen et al. 2005), even those at distances further than 100 parent crater radii exhibit lower depth/diameter ratios than expected for similarly sized primaries.

There are several possible explanations for lower depth/diameter ratios of secondaries:

1. The rise time of the pressure or shock wave, a function of the time required for the projectile to travel its radius into the target and deliver its energy and momentum, is longer for the lower-velocity secondaries. The longer rise time broadens the wave, reducing the peak pressure and thus diminishing the excavation flow for a secondary crater. Apparently the lower velocity enables the momentum (proportional to v) to preserve directionality in the face of the scalar kinetic energy (proportional to v^2), meaning that secondary craters created by low-velocity ejecta exhibit elliptical outlines more often than primaries.
2. Schultz & Gault (1985) investigated the effect of clustered projectiles (which may be common in ejecta) on crater morphology. They found that as dispersion increases from a single intact projectile to a distributed group on impact, the resulting feature changes from a simple, bowl-shaped crater to a progressively shallower crater.
3. In simultaneous formation of a cluster of secondary craters, the ejecta interacts, leading to ballistic erosion and sedimentation that destroys the smallest

craters and partially fills in larger craters, thus reducing depth/diameter ratios (Oberbeck 1975).

RELATIVE PRIMARY VERSUS SECONDARY CRATER ABUNDANCES

Should we expect distant secondary craters to be relatively more or less common on Mars or Europa than on the Moon? Primary impact velocities are lower on Mars, and secondary impact velocities can be higher (up to 5 km s^{-1} escape velocity versus 2.4 km s^{-1} for the Moon or 2 km s^{-1} on Europa), but ejecta of a given velocity travels further on the less-massive bodies. Mars and especially Europa have significant surface areas with little regolith, where even small impacts produce abundant high-velocity spalls (Melosh 1984, Head et al. 2002). The atmosphere of Mars must reduce the density of small primary craters and flatten the SFD below some diameter limit (Melosh 1989, Chappelow & Sharpton 2005). Because the criterion for a projectile to break up in the atmosphere is proportional to velocity squared, the Mars atmosphere should have less of an effect on the lower-velocity blocks larger than 10 cm diameter that produce secondary craters, even though they may pass through the atmosphere twice. Ejecta fragments smaller than 10 cm are significantly decelerated by Mars' current atmosphere on their way up (Artemieva & Ivanov 2004).

Europa is different from both the Moon and Mars because its surface is mostly water ice, which is weaker than silicate rock (it has lower compressional and tensional strengths) and a lower melting temperature. Thus an impact of a given kinetic energy produces a larger crater in an icy target than in a rocky target (Fink et al. 1984). Laboratory evidence reveals that impacts into ice generate more fragments than equivalent impacts into rock (Kato et al. 1995, 2001; Arakawa et al. 1995). Perhaps the major difference is that small primary craters are produced at a much lower frequency on Europa (Chapman et al. 1997, Zahnle et al. 2003) than on the Moon and Mars, so the fraction of small craters that are secondaries may be much higher than primaries.

Although measurable factors contribute to different secondary crater production efficiencies between bodies, these differences (though currently not well quantified) cannot be used to suggest that secondaries are dominant on one surface but not another (for objects with comparable, within a factor of a few, surface gravity). The basic physics of crater formation, excavation, and ejecta distribution are the same in solid, semi-infinite targets. Variations in target strength, porosity, layering, impact angle, and projectile type all affect the particulars of an individual impact and contribute to differences in ejecta mass by factors of several, but the bulk characteristics are similar. And these factors of several are well below the several-orders-of magnitude difference in crater density between primaries and secondaries suggested by recent results (Bierhaus et al. 2005, McEwen et al. 2005). Thus although we must acknowledge and consider the differences between objects in secondary populations (or even different terrains on the same object), we conclude that secondary craters may dominate the small-crater populations (below some crossover diameter) over most of the Moon, Mars, and Europa.

A 40-YEAR-OLD LUNAR CONTROVERSY

The origins of small (less than ~1 km diameter) lunar impact craters were controversial following the first successful Lunar Ranger missions in the 1960s. E.M. Shoemaker (cf. Levy 2000) and colleagues interpreted the majority of such craters as secondaries, and a secondary origin was soon widely accepted for craters that were formed close to the primary and that were organized into tight chains and clusters with distinctive morphologies. The relative abundance of distant secondaries was more controversial, in spite of the obvious bright rays extending thousands of kilometers from recent large craters such as Tycho.

Saturation equilibrium: steady-state condition in which each new crater obliterates, on average, another crater of equal size, so the complete cratering record cannot be determined

The SFD of craters over limited size ranges is commonly described by a power law of the form $N(\geq D) = kD^{-b}$, where N is the cumulative number of craters, D is crater diameter, k is a constant that depends on crater density, and b is the absolute value of the power-law exponent. We also refer to this negative exponent as the slope. The SFD can also be presented as the differential number of craters (add 1 to the value of b to compare with the cumulative SFD), or in the logarithmic-differential format (Hartmann et al. 1981) (same value of b as cumulative distribution except near changes of slope). There is also the R format in which the differential data is divided by a power-law function with b (differential) equal to three. In this review we use b values appropriate for the cumulative or logarithmic-differential plots for ease of comparison with much of the crater literature, and we note that differential data must be used to derive accurate SFD slopes (Chapman & Haefner 1967). Primary craters on the Moon and Mars with diameters from approximately 1 to 100 km have $b \approx 2$ (Hartmann et al. 1981), whereas secondary craters produced by a single primary crater (on the Moon, Mars, and Europa) have a steeper SFD with $b \approx 3.5$–5.5 (Shoemaker 1965, Wilhelms et al. 1978, Bierhaus et al. 2001, McEwen et al. 2005). The SFDs of the lunar maria and other plains, excluding obvious secondaries, show a steeper slope (b ~ 4) for craters smaller than ~1 km (**Figure 2**). Shoemaker (1965) presented a hypothetical model in which ~1 km is the crossover diameter between two distributions: Primaries (with $b = 2$ at all sizes) dominate for craters larger than ~1 km and secondaries (with $b \approx 4$) dominate at smaller sizes. Shoemaker measured the SFD of secondary craters from the Sedan nuclear-explosion crater in Nevada (**Figure 3**) and several lunar craters. He noted that the crossover diameter should vary as a function of proximity to crater rays. Away from known lunar crater rays, Shoemaker estimated that distant secondaries should dominate at crater diameters smaller than ~200 m, and he preferred a model of the primary production function that steepened to $b \approx 3$ at diameters less than ~1 km. Shoemaker's favored model is difficult to test on the Moon because the lunar maria reached a steady-state SFD (Shoemaker 1965), or saturation equilibrium (Hartmann & Gaskell 1997) at sizes smaller than ~250 m, and few craters larger than 100 m are present on the young surfaces (which are not in saturation equilibrium) produced by large Copernican craters (Neukum & Koenig 1976, McEwen et al. 1993).

Studies of the Moon (e.g., Guinness & Arvidson 1977, Wilhelms et al. 1978) and Mars (e.g., Soderblom et al. 1974, Tanaka 1986, Strom et al. 1992) reflected Shoemaker's interpretation that secondaries dominate the cratering statistics below

Figure 2

Size-frequency distribution of typical lunar maria. The straight solid line represents a model for saturation equilibrium. Data from Hartmann et al. (1981, p. 1114, plot 11).

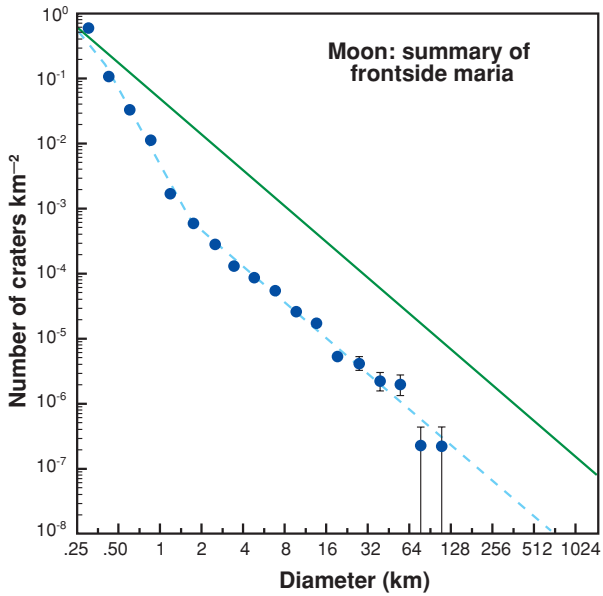

Figure 3

Aerial photograph of the ~400-m diameter Sedan nuclear-explosion crater in Nevada. Shoemaker (1965) reported that more than 5000 secondaries from 2–32-m diameter are resolved in the original photograph, but that smaller craters are also present. Roberts (1964) estimated than Sedan produced tens of thousands of secondary craters.

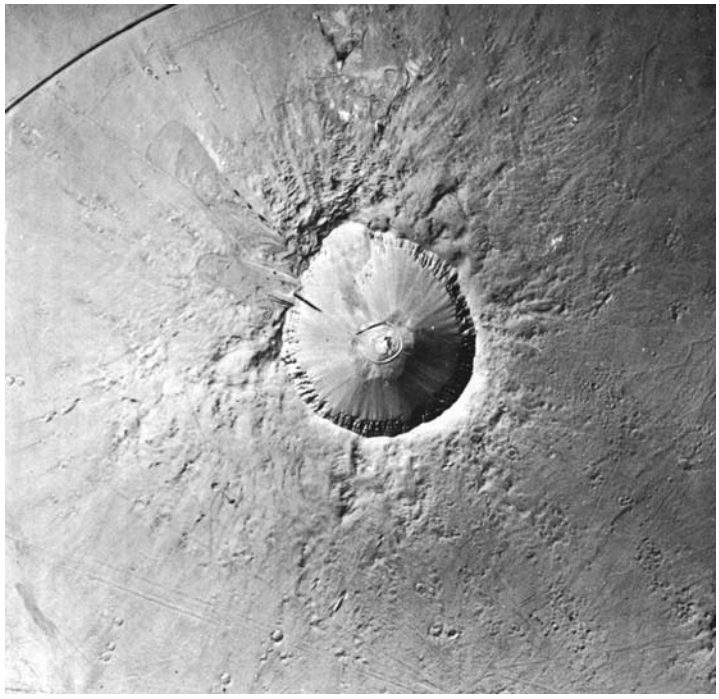

a crossover diameter, whereas others believed that small circular craters without herringbone patterns were chiefly primaries (e.g., Neukum et al. 1975, Moore et al. 1980). The observation of a relatively steep SFD (*b* from 3.1 to 3.7) for small craters (~0.2 to 1 km) on the asteroid Gaspra (Chapman et al. 1996), where secondary craters are not expected due to the very low escape velocity, was considered strong evidence for a steep primary SFD for craters smaller than 1 km (Neukum & Ivanov 1994, Neukum et al. 2001). However, the Galileo observations of Gaspra did not provide reliable information on the SFD of craters smaller than ~200 m, and as a main-belt object, Gaspra has a cratering history different from that of the Moon or Mars, which are hit by near-Earth projectiles. Most significant, perhaps, is the affect of the mass-velocity distribution of projectiles, which we discuss in the section Why the Majority of Small Impact Craters are Secondaries, below.

Many researchers have been convinced that small craters on the terrestrial planets, aside from obvious secondaries, are dominated by primaries; they have also assumed that the production function of small primary craters is well known. In recent reviews, secondaries are dismissed as unimportant (Neukum & Ivanov 1994) or not even mentioned (Hartmann & Neukum 2001, Neukum et al. 2001, Ivanov et al. 2002). Many recent publications (especially about Mars) use small craters for age dating (e.g., Hiesinger et al. 2003, Mangold 2003, Werner et al. 2003, Quantin et al. 2004, Reiss et al. 2004, Neukum et al. 2004, Arfstrom & Hartmann 2005, Basilevsky et al. 2005, Hauber et al. 2005, Murray et al. 2005). The issue is not just that secondaries may contaminate the counts, but that the production functions used by these researchers may greatly overpredict the production rate of small primary craters, as secondary craters have shaped the small-diameter end of the production functions. There has been some confusion over this point (e.g., Hartmann 2005).

SECONDARY REVIVAL

The discoveries on Earth of meteorites from the Moon (Warren et al. 1983) and Mars (reviewed by Nyquist et al. 2001) indicate that distant secondary craters on these bodies must be significant. Head et al. (2002) estimated that the probability that a rock ejected from Mars will land on Earth and be discovered is 10^{-6} to 10^{-7}. Thus an impact event that delivered a discovered meteorite to Earth must have ejected at least 10^6 rocks larger than 3 cm in diameter at greater-than-Mars escape velocity. The hydrocode modeling of Head et al. (2002) indicates that the vertical impact of a 150-m-diameter projectile (producing a 3-km-diameter crater) into basaltic plains with negligible regolith will eject $>10^7$ fragments larger than 3 cm (ignoring atmospheric deceleration). This is a small fraction of the high-velocity (>1 km s^{-1}) ejecta; most fragments must fall back onto Mars. The negative correlation between fragment size and ejection velocity means that most of the larger high-velocity fragments turn into distant secondary craters rather than escape Mars. In an oblique impact, the amount of high-velocity ejecta in the downrange direction increases by an order of magnitude (Pierazzo & Melosh 2000, Artemieva & Ivanov 2004, Yamamoto et al. 2005). Such high-velocity fragments can land over widespread regions.

Renewed international interest in lunar exploration has motivated some recent research relevant to secondary cratering. An effort to test hypotheses for the origin of small lunar craters by Namiki & Honda (2003) is of special interest to this review. They determined SFDs designed to test four hypotheses for the steep branch of the mare SFD and found two of them (endogenic craters and effects of the near-surface stratigraphy) easy to dismiss. The two remaining hypotheses involve a steepening of the primary production function and the effect of secondary craters. They concluded that a steepening of the primary production function failed to explain the wide variation of SFDs measured within geologic units. The secondary origin was favored in part by process of elimination, but also because of strong gradients in small-crater density with radial distance from Aristarchus (40 km diameter) and Diophantus (18 km diameter), extending as far as 15 crater diameters from the primary. However, the gradient is not strong or extended around all craters, e.g., around Bessel (16 km diameter), as determined by Neukum et al. (1975). Some primary craters probably produce many more secondaries than others, owing to the impact angle and other factors. However, if even just 10% of the large craters produce large numbers ($>10^6$) of secondaries, it could have a significant effect on the global power-law crater SFD.

A major limitation to fully understanding secondary cratering has been the limited extent of young terrains on the Moon (i.e., those not in saturation equilibrium) and the absence of high-resolution imaging of other bodies. This situation has been remedied by sampling Europa's entirely young surface by Galileo and by imaging young regions of Mars by Mars Global Surveyor and other spacecraft missions.

RECENT RESULTS FROM EUROPA

Galileo images confirmed the Voyager-era impression that Europa has few large craters. To date, there are less than 24 craters with diameters $\geq$10 km identified in moderate- and low-resolution global imagery (Schenk et al. 2004). Zahnle et al. (2003) used the dynamical simulations of Levison et al. (1997, 2000) to calculate an average surface age of approximately 60 million years. The first high-resolution images revealed a population of small craters far more numerous than expected from extrapolating the large-crater SFD to diameters less than 1 km. Bierhaus (2004) identified more than 17,000 craters in the high-resolution mosaics (scales $<$60 m pix^{-1}), which cover only 0.2% of Europa's surface. Assuming these random samples are typical, there must be $\sim 10^7$ craters from 0.2 to 1.0 km diameter on Europa. The number of small craters measured increases to more than 27,000 when the near-field secondaries around the primary craters Tyre and Pwyll are added. The small craters demonstrate two characteristics regardless of location on Europa: (*a*) Many, if not most, of the craters are in spatial clusters (e.g., **Figure 1**); and (*b*) the crater size distributions are steeply sloped; most have a cumulative power-law size index of $b > 3$.

Bierhaus et al. (2001) and Bierhaus (2004) analyzed two image sequences that transect a bright ray from the ~25-km-diameter Pwyll crater (thought likely to be Europa's youngest large crater because of the presence of an extensive and prominent ray system; **Figure 4**). The two regions are ~1000 km and ~1200 km from Pwyll (the ray extends at least a few hundred kilometers further); they contain numerous Pwyll

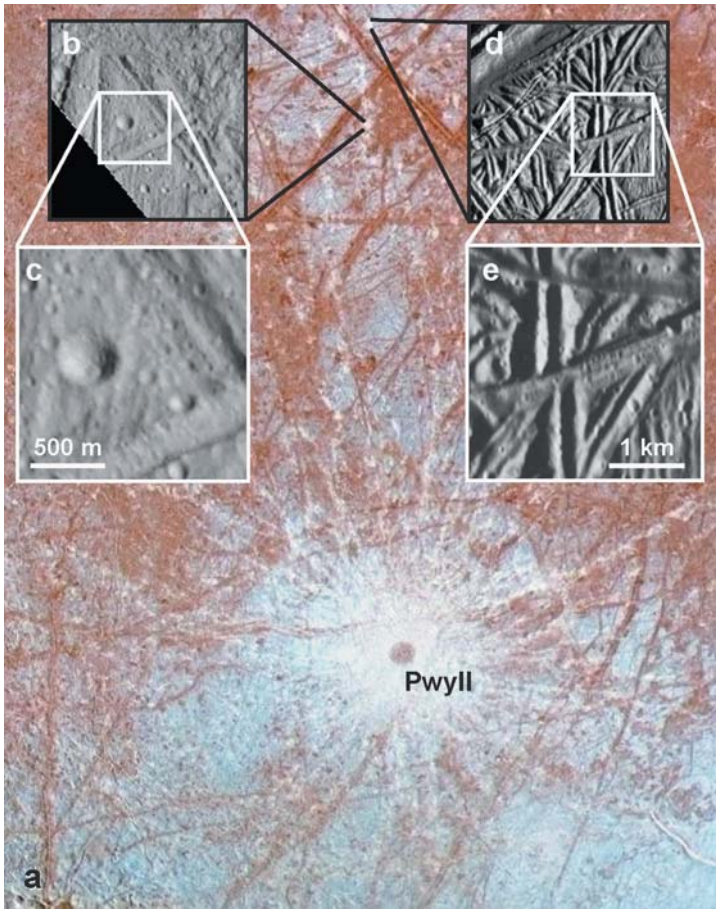

Figure 4

(*a*) An enhanced-color, regional mosaic that shows the impact crater Pwyll and its extensive ray system. (Note that the 25 km diameter Pwyll is smaller than the dark center of the bright ray system.) (*b*) A portion of the western side of the ~10 m pixel^{-1} image sequence E12CHAOS_01, which is within a Pwyll bright ray. (*c*) A zoomed-in portion of (*b*) that better shows the extensive Pwyll secondary crater population. This region is about 1000 km from Pwyll. (*d*) A portion of the ~20 m pixel^{-1} image sequence E06BRTPLN02, also within a bright ray patch. (*e*) A zoomed-in portion of (*d*) that shows the numerous Pwyll secondaries in this region.

secondaries, 3300 craters with diameters larger than the size limit at which the counts are complete. These regions are just two points along a single ray, with a combined area of approximately 1250 km^2. Integrating the number of secondaries along their parent ray could accumulate at least two orders of magnitude more craters, as there are tens of thousands of square kilometers covered by the ray between these mosaics and Pwyll (assuming an average ray width of 30 km). And this is just a single ray—tens of other rays similarly extend thousands of kilometers away. If the crater density within other rays is similar, Pwyll may have generated several million secondaries larger than 100 m in diameter.

Three spatial analyses (Z-statistics, K-functions, and Monte Carlo simulations) demonstrate that Europa's small-crater population is strongly clustered. To remove the strongly clustered craters, to estimate the spatially random background, and to identify specific clusters, Bierhaus et al. (2005) developed a technique that employs the single-linkage (SLINK) hierarchical clustering algorithm, Monte Carlo simulations,

and a parameter that estimates the degree of clustering for each crater. This technique divides the crater population into groups by probabilities P of nonrandomness, where a cluster with $P > 2\sigma$ indicates that the cluster is nonrandom [with significance greater than 2 standard deviations (2σ or 95%)] and thus has only a 5% chance of occurring by random impacts. Among nine high-resolution mosaics, the minimum, maximum, and median percentage of craters clustered at $P > 2\sigma$ are 35%, 80%, and 71%, respectively. (Fielder et al. 1972 conducted spatial analyses on craters seen in Lunar Orbiter images and concluded that several regions contained significant clustering. However, they rejected the secondary crater hypothesis because of "no apparent relation to the largest craters in the vicinity.")

The shapes (i.e., the parameter b) of the SFD for spatially random craters mimic that of the strongly clustered craters on a region-by-region basis. The divergent SFDs of the unclustered craters are not consistent with a single-source SFD, e.g., primary projectiles. Because b for the spatially random craters varies regionally, mimicking the regional variations of the strongly clustered craters, many, if not most, of the unclustered craters may also be secondaries. The combined analyses of clustered craters and the similar SFDs of spatially random craters indicate that ~95% of Europa's small craters are secondaries (Bierhaus et al. 2005).

Secondary craters close to their primaries have very steep size distributions. Secondaries around Pwyll have a cumulative power-law index of -4.5 ± 0.9, whereas secondaries around Tyre have a power-law index of -4.2 ± 1.0. The very steep best-fit values may indicate that these secondaries form by a different process than the distant secondaries, but the error bars on both populations prohibit a definitive statement one way or the other.

Several important implications stem from the Europa results:

- The production and distribution of secondary-producing ejecta is extensive. The few dozens of large Europa impact craters are enough to generate tens of millions of secondaries larger than 200 m diameter; the steep SFD suggests yet more secondaries at diameters below the resolution limits of the available data.
- If a few large primary craters can generate a globally extensive network of secondaries, then more heavily cratered surfaces (e.g., the Moon and Mars) must bear the imprint of incredible numbers of secondaries, assuming that secondary generation is as efficient for these targets.
- The Pwyll example demonstrates that far-flung secondaries (more than 1000 km distant from their primary crater) can dominate the local crater population. Measuring populations that are located far from a large primary may be a way to minimize the contamination of secondaries, but the potential presence of secondaries will never be eliminated unless there are terrains that are known to be younger than the most recent secondary-forming primary impact.
- Finally, because the SFD from primaries is expected to be nearly the same everywhere on Europa, the measured variability of the SFD of the spatially random population indicates that it is significantly contaminated by secondaries.

Both Ganymede and Callisto exhibit steep branches in their crater SFD, beginning at a few kilometers in diameter. Because they represent longer integration times

of the same projectile population that strikes Europa, they serve as a useful check on the Europa results. Initial evidence for both objects suggests that secondaries are the source of the steep crater SFD. The Osiris crater on Ganymede is one of many craters with an extensive and bright ray system correlated with crater clusters over a large area of Ganymede's surface. Callisto's small-crater population (<1 km diameter), as measured in the few images with sufficient resolution and quality for crater measurement, demonstrates a strong steepening of slope relative to larger diameters. Bierhaus (2004) showed a discrete set of small-crater erosional states within a region, consistent with all of the craters forming in a small number of secondary events, rather than a continuous production via primary cratering.

RECENT RESULTS FROM MARS

McEwen et al. (2005) reported rays of secondary craters extending as far as 1600 km from the 10.1-km diameter crater Zunil in the young volcanic plains of Cerberus (Elysium Planitia) (**Figure 5**). This was the first discovery of a large rayed crater on Mars. Tornabene et al. (2005) described four additional Martian rayed craters, and three others that are probably faded rayed craters, with diameters from 1.5 to 7.4 km. These rays, like those of Zunil, contain dense concentrations of secondary craters. All of these rays [including those from Zunil (Preblich et al. 2005)] are seen from temperature contrasts in nighttime infrared images from the Thermal Emission Imaging System (THEMIS), but only over terrains with intermediate thermal inertia and albedo (e.g., Mellon et al. 2000), which cover ~20% of Mars. This suggests that similar ray-forming events have occurred elsewhere on Mars, but without either temperature or albedo contrasts, the only way to map the rays is to map the distributions of secondaries.

Zunil provides a well-preserved example of a primary crater with enormous numbers of distant secondary craters. This event created $\sim 10^8$ secondary craters from 10–100 m diameter, with a SFD slope over portions of the rays as steep as –5.5 (Preblich et al. 2005). There are very few secondary craters within ~16 crater radii; they were almost all formed at greater ranges, so there are none of the obvious adjacent secondary craters that are routinely excluded from crater counts for age dating. Zunil is a plausible source crater for some of the Martian meteorites (basaltic shergottites) with lava emplacement ages of 165–177 Ma and ejection ages of either ~1.5 or ~2.7 Ma (Nyquist et al. 2001).

A simulation of a Zunil-like impact ejected $\sim 10^9$ rock fragments capable of forming distant secondary craters ≥10 m diameter (McEwen et al. 2005, Artemieva 2005). According to the simulation, ~70% of the craters larger than 10 m diameter form at distances of 800 to 3500 km, whereas most craters larger than 50 m form within 800 km of the primary, in close agreement with results from Preblich et al. (2005). If the secondary crater production of Zunil is not highly unusual, then the total number of small craters on Mars is easily accounted for as distant secondaries.

Is Zunil typical or unusual as a producer of secondary craters? Zunil formed on the youngest large-scale lava plains on Mars, perhaps an ideal location for spallation. The thicker the regolith layer relative to projectile radius, the greater the reduction

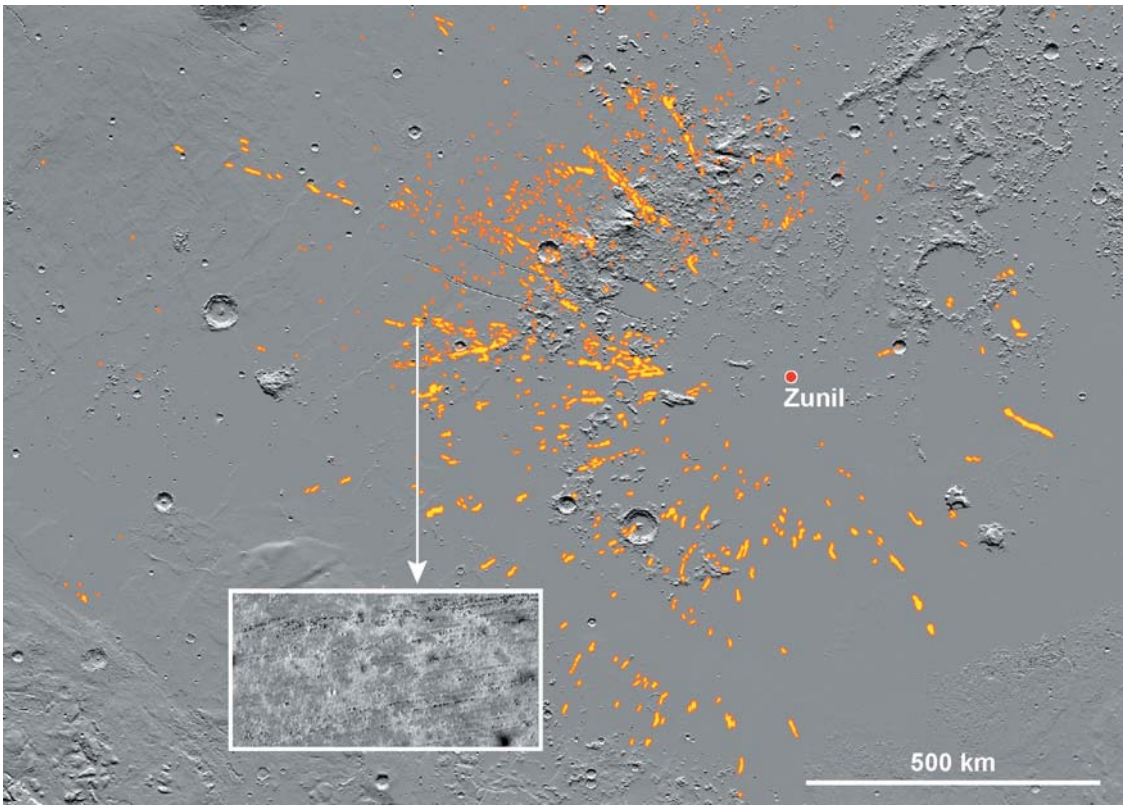

Figure 5

Map of Zunil rays seen in THEMIS nighttime infrared mosaic (Preblich et al. 2005), superimposed over a shaded-relief map from the Mars Orbital Laser Altimeter (MOLA). Ray areas are yellow, but outlined in orange to improve visibility. Zunil is indicated in red. Rays are not seen in THEMIS nighttime infrared data when superimposed over terrains with very low thermal inertia (due to dust cover), but secondary craters are seen in high-resolution MOC images. Thermal inertia is very low around Zunil and to the east, except in isolated areas, but there does seem to be a real asymmetry, consistent with an oblique impact from the east. The most distant ray segments, 1700 km west of Zunil, are clipped in this view, as is a region of probable Zunil secondaries (not in rays) extending up to 3500 km to the west. The inset shows a small portion of MOC image MO2-00581 (5.9 m pixel^{-1}) over a ray segment of Zunil (beginning of arrow). There are ~100 craters larger than 20 m diameter in this small area (1.5 × 3 km).

in peak spall velocity (Head et al. 2002), but large impacts may produce significant distant secondaries even on heavily damaged ground. For example, Tycho (85 km diameter) formed over the brecciated highlands of the Moon, yet formed more than 10^6 secondary craters larger than 100 m diameter within rays longer than 1000 km (Dundas & McEwen 2005). Only relatively small primary craters (<10 km diameter, <100 m projectiles) over ancient terrains with thick regolith or terrains with a thick low-density sedimentary mantle are expected to produce few distant secondary craters

by spallation. Obliquity of the impact may be the major factor determining the number of distant secondary craters produced, and the ejecta pattern of Zunil suggests a typical obliquity, probably between 30° and 60°.

McEwen et al. (2005) described several lines of evidence indicating that secondaries dominate the numbers of small craters on Mars:

1. Measurements of 1300 small craters over Gusev crater and Isidis Planitia show that the small craters have depth/diameter ratios of ~0.11 or less, similar to lunar secondary craters (Pike & Wilhelms 1978) and much shallower than expected for primaries, except perhaps on highly porous targets.
2. The fine-layered deposits on Mars are probably billions of years old (Malin & Edgett 2001), yet are largely free of small craters, owing to wind erosion. If the small craters are primaries that form randomly in time, the erosion rate required to remove the most recent craters would have eliminated the deposits in less than 10^8 years. The contradiction in age is eliminated, and the deposits can be billions of years old, if the cratering is strongly clustered in time, as expected from secondary cratering.
3. The regolith thicknesses at three past landing sites (Viking Landers 1 and 2, and Pathfinder) appear to be far less than predictions from the Hartmann/Neukum production functions, suggesting that primary craters smaller than 60 m form less often than predicted by these production functions.

The strongest evidence that the primary production function for small Martian craters must be less than predicted comes from age contradictions derived from small versus large craters. Age estimates on three large (10, 23, and 29 km) craters based on Hartmann/Neukum production functions require three highly improbable (<0.1%) events in the past 10–100 Ka. Alternatively, these production functions predict too many small primary craters. Atmospheric filtering or aeolian processes cannot adequately explain the discrepancy (McEwen et al. 2005), so these numbers probably reflect the size distribution of small bodies ejected from the asteroid belt that cross the orbits of Mars and Earth (Bottke et al. 2005). Bierhaus et al. (2005) applied the secondary-cratering efficiency (the amount of ejecta generated for a given energy primary impact) they measured on Europa to the Moon and found that the secondaries generated by the postmare impact population with 10 km $< D <$ 64 km could account for the Moon's <1 km diameter crater population, even if lunar craters generate several times fewer secondaries than Europa. We conclude that the Hartmann/Neukum production functions must be heavily contaminated by secondary craters and overpredict the production of small primary craters.

A wonderful close-up example of a distant secondary crater that could easily be mistaken for a degraded primary is Bonneville, explored by the Mars Exploration Rover (MER) Spirit (Grant et al. 2004) (**Figure 6**). From orbit, Bonneville looks like a typical degraded primary crater, but it must be morphologically pristine because the ejecta blanket is well preserved, and the eolian infill is thin. Bonneville formed in basaltic plains, where a depth/diameter ratio of ~0.2 is expected for primary craters, but instead, because its depth/diameter is 0.07, the MER Spirit team interpreted it

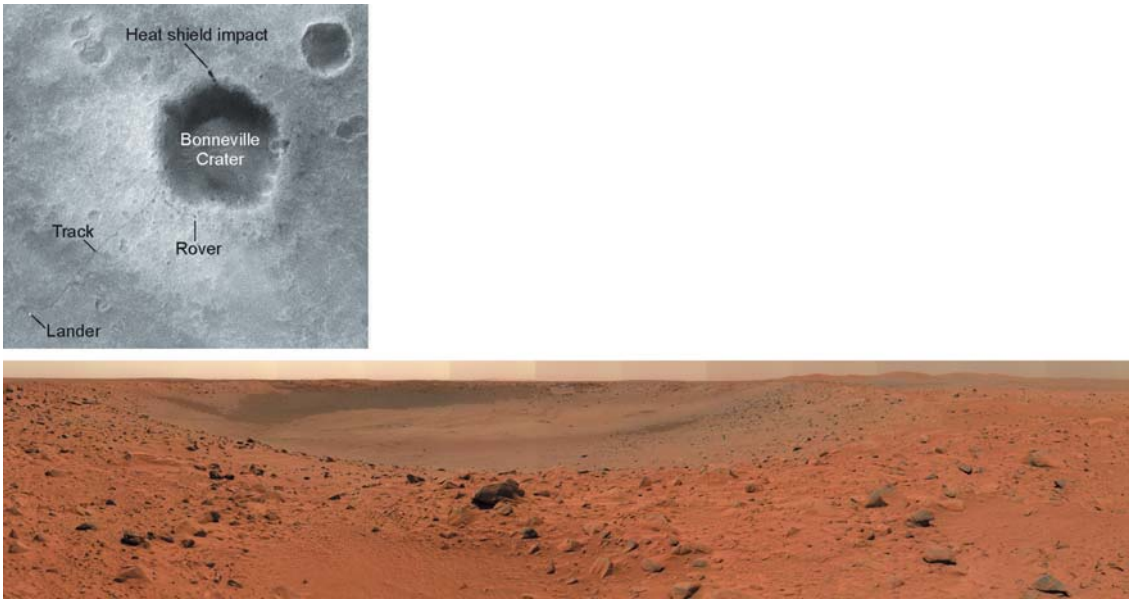

Figure 6

(*Top*) Orbital view of the Bonneville crater from the MOC (image from http://www.msss.com). (*Bottom*) View from the ground of Bonneville from the MER Spirit Panoramic Camera. Crater diameter is 210 m.

as a relatively pristine secondary crater. There is no plausible nearby source crater, so it must be a distant, unclustered secondary crater.

Interplanetary debris: icy, rocky, or metallic material that crosses the orbit of a planet but originated outside that planetary system

WHY THE MAJORITY OF SMALL IMPACT CRATERS ARE SECONDARIES

Secondary craters have a steeper power-law SFD than primaries, so they rapidly catch up to and exceed the numbers of primary craters below a certain size. But why is the SFD steeper? Impacts into asteroids create most of the interplanetary debris in the inner Solar System, so the SFD of the fragments generated by a primary impact on a planetary surface and the fragments generated during inter-asteroid collisions may be similar (Hartmann 1969); Hartmann (2005) wrote, "it remains to be shown that the size distributions would be seriously different." Although the SFD of the fragments may be similar, that does not mean the SFD of the craters will be similar.

There is a strong inverse correlation between the average size and average velocity of impact ejecta fragments, [perhaps best explained by the physics of spallation (Melosh 1984)], and it is this correlation that has a vital role in explaining the steep SFDs of secondary craters and why they dominate the numbers of small craters. If the same SFD of fragments was ejected independent of velocity, then secondary craters would get larger (on average) as they formed further from the primary, as they impact

at higher velocities at greater distances. In actuality secondary craters get smaller (on average) or remain roughly constant in size with respect to distance from the primary crater of origin (Schultz & Singer 1980; Vickery 1986, 1987; Hirase et al. 2004; Preblich et al. 2005). In this section we present calculations to demonstrate that the inverse size-velocity correlation could markedly steepen the SFD of resulting craters. We believe that the size-velocity relationship fundamentally explains why secondary craters have a steeper SFD than do craters produced from interplanetary or planetocentric debris. The SFDs of both primaries and secondaries are power-law functions, so even a small difference in slope means that the steeper-sloped distribution must eventually "win the race" and become more numerous than primaries below the crossover diameter.

Shoemaker (1962) first proposed that secondary craters form from spallation of the surface layer. Melosh (1984) predicted a size-velocity relationship for the largest fragments, with a numerical model for impact spallation. The relationship has been measured from studies of secondary craters and from laboratory experiments (Vickery 1986, 1987; Polanskey & Ahrens 1990; Nakamura & Fujiwara 1991; Nakamura et al. 1994; Hirase et al. 2004; Onose & Fujiwara 2004). The significance of the size-velocity relationship to the primary versus secondary crater controversy has not been noted, to our knowledge, until recently (N. Artemieva, oral presentation at 2005 Lunar and Planetary Science Conference).

Melosh's model gave similar size-velocity predictions for impact velocities of 10 and 20 km s^{-1} (table 2 of Melosh 1984). For ejecta velocities from ~0.5 to 5 km s^{-1}, relevant to fragments that fall back to make distant secondary craters on the Moon, Mars, and Europa, the dependence is close to $\log(V_{spall}) = -1.2\log(D_{spall}/a) - 1.5$ (see figure 8b of Melosh 1984), where V_{spall} is ejection velocity of the largest fragments, D_{spall} is its diameter, and a is the mean radius of the projectile. The model falls within the scatter of data points shown by Vickery (1986) and provides a means of extrapolation to higher velocities. Spallation is not necessarily the only origin for the nearby to intermediate-distance secondaries, which come from the bulk excavation flow post spallation. Regardless of the exact mechanism(s), a definite size-velocity relationship has been measured in the laboratory and inferred from secondary craters.

Some simple calculations demonstrate how the crater SFD can be markedly influenced by the size-velocity correlation. To calculate how impact velocity affects the diameter of lunar craters, we used the scaling relations of Holsapple and others (**http://keith.aa.washington.edu/craterdata/scaling/index.htm**) (see Housen et al. 1983 and Holsapple 1993) to model the diameters of small lunar craters impacting into bed rock (lunar maria). The numerical experiment compares the crater SFD generated by primary projectiles with the crater SFD generated by secondary projectiles, assuming the same impactor SFD for the primary and secondary projectiles. The results of these calculations are given in **Table 1**. First, we calculated the crater diameters produced by interplanetary fragments from 30 to 90 m diameter at 15 km s^{-1}, 45° impact angle, with a SFD slope of –2 (**Table 1*a***). Next, we calculated the ejecta fragment velocities (for the same SFD of fragments) created by a primary impact at ~15 km s^{-1} from our linear approximation of Melosh's model, then

Table 1 Effect of projectile size-frequency distribution ($b = 2$) on lunar crater size–frequency distribution (see Figure 7)

(*a*) Interplanetary projectiles (all impacting at 15 km s^{-1})			
$D_{fragment}$ (m)	Number of fragments	D_{crater} (m)	
30	90	518	
40	50.6	674	
50	32.4	824	
60	22.5	969	
70	16.5	1110	
80	12.6	1250	
90	10	1380	
(*b*) Spall projectiles from large primary craters			
$D_{fragment}$ (m)	Number of fragments	Impact V (km s^{-1})	D_{crater} (m)
30	90	1.8	173
40	50.6	1.3	190
50	32.4	1.0	205
60	22.5	0.8	219
70	16.5	0.7	232
80	12.6	0.6	242
90	10	0.5	251

recalculated crater diameters produced by secondary impact at those velocities, again at a 45° impact angle (**Table 1*b***). Secondary craters of this size and impact velocity require a primary crater ~20 km diameter.

At a constant interplanetary impact velocity of 15 km s^{-1}, the range in crater diameter in **Table 1*a*** is a factor of 3.9, which is slightly greater than the range in fragment diameter, so the SFD slope of the resulting craters is –2.2. However, the same-sized fragments, produced via spallation from a primary impact, generate craters that vary in size by a factor of just 1.4. This produces a marked steepening of the SFD to a slope of –5.8 (**Figure 7**), which is even steeper than that typically seen for secondary craters of Zunil and Pwyll, which may have formed in near-ideal targets for spallation. This steepening may be an upper limit, as Melosh's model applies to the largest fragments. Also, this example is oversimplified because there is actually a distribution of fragment sizes at any velocity, we do not account for the destruction of small craters during the formation of dense secondary clusters, and we do not account for the effects of regolith. In addition, the actual size-velocity relationship is poorly known for velocities above 1 km s^{-1}, both from measurements and in the theoretical model of Melosh (1984).

Further work is needed, but this example demonstrates that secondary craters should have a steeper SFD than small primary craters, perhaps much steeper, even if the projectile SFD is the same between primary and secondary populations. Ejecta that escape from asteroids and eventually reach the Moon or Mars have velocities controlled by orbital dynamics, and no size-velocity dependence from the original impact is retained.

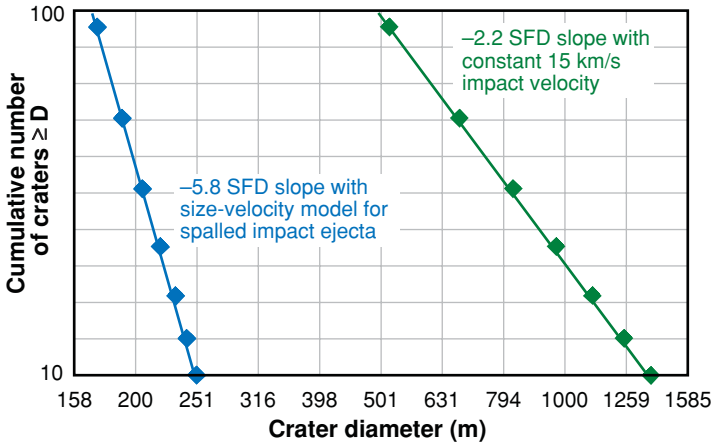

Figure 7

Steepening of crater size-frequency distribution (SFD) owing to size-velocity dependence of ejecta fragments producing secondary craters. Impacting objects range from 30–90 m diameter in both cases. Diameters showing –2.2 SFD slope are calculated for primary impacts at 15 km s^{-1} on the Moon, whereas those with –5.8 SFD slope are calculated for impact velocities expected from the spallation fragments produced by 10–20 km s^{-1} impacts (see **Table 1**).

WHAT ARE THE PRIMARY PRODUCTION FUNCTIONS FOR SMALL CRATERS?

At least three different approaches have been taken to address the issue of primary production functions for small craters on the Moon and Mars. Hartmann (1970) measured a SFD slope of −3.8 on the lunar maria for crater diameters from ∼300 m to 1 km. Saturation equilibrium flattens the slope for craters smaller then 300 m on the lunar maria, so Hartmann (1999) extrapolated the −3.8 SFD slope to smaller diameters. Neukum et al. (1975, 2001) measured the SFD at smaller sizes over the deposits from large Copernican craters, where saturation equilibrium has not occurred, and found that the SFD flattened somewhat at small sizes. In both cases the production function for craters smaller than 1 km was steep, similar to the measured slope of secondary craters. Both researchers then assumed the same projectile SFD cratered Mars and scaled the lunar production functions to Mars, accounting for the differences in gravity, mean impact velocity, and overall flux rate (Ivanov 2001).

The third approach is to try to determine the production function while avoiding distant secondary craters as carefully as possible (Guinness & Arvidson 1977, Moore et al. 1980, Plaut 2005). Extremely young surfaces should be largely free of secondaries unless there is a younger large crater nearby, although there is no guarantee that distant secondaries are absent. Tycho (85 km diameter) is anomalously large for an impact event ∼109 million years old (Arvidson et al. 1976, Drozd et al. 1977), so it may be relatively lightly cratered by distant secondaries. Guinness & Arvidson (1977) measured the SFD of small craters superimposed on deposits of Tycho, a lightly cratered unit on the floor of Copernicus, and a region surrounding the Apollo 12

landing site, origin of the youngest crystallization ages (3.26×10^9 years) of basalts in returned samples. They made a concerted effort to avoid distant secondaries by plotting out the direction towards large craters that are younger than the terrain in question, although this did not eliminate all possible secondaries. At all three locations they measured $b \sim 2.7$. The counts on Tycho extend to as low as ~30 m, well below the diameter of saturation equilibrium on the maria. For craters 5–50 m diameter, Moore et al. (1980) measured SFDs with b of 2.8 and 2.75 on the well-dated North Ray crater (50 million years) and Cone Crater (24 million years) (Arvidson et al. 1975), respectively. Slopes of 2.7–2.8 are lower than the 3.8 measured by Hartmann (1970, 1999) for larger craters and are flatter than the curve over most of this size range reported by Neukum et al. (1975, 2001).

There is also evidence for a shallower primary production function on Mars. There are young terrains on Mars where the contribution of secondaries may be minimal, such as the south-polar layered terrain (~10 million years old on the basis of large craters), where Plaut (2005) found $b = 2$ down to 300 m diameter craters. The SFD slope becomes shallower owing to erosion and deposition, preferentially erasing small craters, so Plaut (2005) counted only those craters with well-preserved original morphologies (circularity, sharp raised rim, and presence of ejecta blanket). Ironically, some past researchers have considered a steep SFD to indicate the primary production function, as erosion has not obviously flattened the assumed distribution. As previously mentioned, McEwen et al. (2005) described three large craters (10–29 km diameter) on Mars whose floors and continuous ejecta blankets are very sparsely cratered. Assuming reasonable ages for these large craters on the basis of large-crater statistics (and the Hartmann/Neukum production function), a small-crater production function that would match observed numbers of small craters (none to a few larger than 20 m superimposed on the large craters) would have $b \approx 2$ for craters from 20 m to 1 km diameter, consistent with the result from Plaut (2005).

Why should we believe that there are probably not significant numbers of distant secondary craters larger than a certain size on especially young surfaces of the Moon and Mars? Secondaries larger than ~0.4% the diameter of the primary are statistically insignificant, of order 10^3, and most of these are obvious adjacent secondaries (Shoemaker 1965, Bierhaus et al. 2001, McEwen et al. 2005, Dundas & McEwen 2005). Thus a significant number of distant secondary craters ≥300 m in diameter require a primary crater larger than 75 km diameter. A crater 75 km or larger has formed somewhere on Mars every 50 million years on average over the past 3.2 billion years (Ivanov 2001). The south-polar layered deposits on Mars are ~10 million years old based on the number of craters >800 m diameter and a conservative ($b = 2$) production function (Herkenhoff & Plaut 2000). There is only ~20% probability that there is a primary crater larger than 75 km anywhere on Mars and younger than the south-polar layered deposits. Furthermore, even a large oblique primary like Tycho deposits secondary craters over much less than 10% of the planet's surface, so the total probability that the south-polar layered deposits have been covered by secondaries larger than 300 m diameter is less than 1 in 50. The global average crossover diameter for a 10–million year Martian terrain should be well below 100 m (McEwen

et al. 2005). Although there is no guarantee that secondaries are absent from young but not zero-age terrains, we do consistently find flatter SFDs on terrains that are unlikely to be significantly contaminated by secondaries.

In summary, evidence from young terrains on the Moon and Mars indicates that the primary SFD for small craters (<1 km) has a flatter slope ($b < 3$) than that for secondary craters ($b > 3$). This result, and the fact that individual primary craters can create millions of secondaries, requires that secondary craters be more abundant as a global average, below some crossover diameter, than small primaries on the Moon and Mars. The key questions for age dating are (*a*) What is that crossover diameter on each particular terrain of interest, and (*b*) What is the detailed shape of the primary production function.

What SFD should we theoretically expect for small primary craters on the Moon and Mars created by debris from the asteroid belt? There is growing recognition (Bottke et al. 2006) of the importance of the Yarkovsky effect (a weak but constant force due to thermal re-emission of sunlight by rotating asteroids) and the YORP (Yarkovsky-O'Keefe-Radzievskii-Paddack) effect of thermal re-emission on spin rates of irregular bodies. These processes affect the orbital evolution and SFD of Earth-crossing asteroids (Morbidelli et al. 2002), such that near-Earth asteroids (NEAs) larger than 1 km (producing craters larger than 10 km) should have a SFD only slightly steeper than that in the main belt (Morbidelli & Vokrouhlicky 2003). Modeling of the effects of thermal re-emission and other processes on the SFD of NEAs smaller than 1 km has recently been completed (Bottke et al. 2005, O'Brien & Greenberg 2005), and both studies conclude that the SFD of small asteroids both in the main belt and NEAs continue to small sizes at a nearly constant slope. These models do not predict significant steepening of the SFD at small sizes, which is needed to explain the Hartmann/Neukum production functions as due to primary craters.

Useful evidence for the SFD of NEAs comes from direct observations, in spite of considerable incompleteness and observational bias (Jedicke et al. 2002). Studies have reported that observed bodies as small as 3 m diameter (Rabinowitz et al. 2000, Brown et al. 2002) agree with the Neukum production function (Werner et al. 2002). However, the crater scaling models of Werner et al. 2002 do not match the data over the full range of observed diameters, so the models are incomplete. Reanalysis of these and other data by Bottke et al. (2005) showed that the observed NEA SFD probably does not explain the steep SFD of craters smaller than 1 km diameter.

Production functions for small craters in the outer Solar System are almost completely unknown, but the paucity of small primary craters on the icy Galilean satellites suggests that small comets are uncommon near Jupiter (Chapman et al. 1997, Zahnle et al. 2003, Bierhaus et al. 2005). In fact, there is no clear evidence for any small primary craters in the outer Solar System, although they must be present to some degree. If a few small impact craters had been detected on Io, where there are no large craters that can be the parent of secondaries, this would constitute direct evidence for small primary craters. In the absence of a plausible production function for small primaries, age dating with small craters is futile in the outer Solar System.

SURFACE AGE CONSTRAINTS FROM SMALL CRATERS

Dating planetary terrains from the densities of superimposed craters is a well-established technique but depends on three key assumptions: (*a*) The craters are independent, random events (i.e., primary craters with statistically insignificant contamination from secondaries), (*b*) the production function SFD for primary craters is known, and (*c*) the cratering rate over time is known. These are relatively safe assumptions for the lunar maria when using craters larger than ~1 km diameter, although at some diameters disagreements up to a factor of five persist for the large-crater production function (Neukum et al. 2001), and the cratering rate over the past 600 million years may have fluctuated by as much as a factor of four (Culler et al. 2000). Secondary craters larger than a few kilometers in diameter are probably very rare on the maria, given the absence of any multiring impact basin larger than 300 km that is believed to be younger than mare surfaces (Wilhelms 1987). Relative age constraints are clearly more reliable than absolute ages. The three key assumptions become increasingly questionable when applied to surfaces where we lack radiometric dates or must use small craters. Error bars are normally shown only for the counting statistics and do not account for the potentially considerable errors that would be present if any of these assumptions were incorrect.

Hartmann (1999, 2005) has argued that counting both the primaries and what appear to be spatially random secondaries is acceptable, but offered no quantitative justification or methodology to define the uncertainties. If most of the seemingly random craters are secondaries, as we believe must often be the case, and if it is possible to determine the number, sizes, and ranges of the primaries that contributed those secondaries, then those few primaries would provide an age constraint with large but quantifiable uncertainties. In practice, this approach may not be achievable.

Concerns about the origins and modification of small craters has led some investigators to completely avoid using craters smaller than ~1 km for age constraints (e.g., Tanaka 1986, Strom et al. 1992, Plescia 2003). However, only small craters are available in significant numbers for crater age constraints on young surfaces or small geologic units. We currently have no other way of remotely estimating ages unless rates of change can be observed or inferred. In this section we discuss the considerable challenges and how researchers can sometimes generate useful age constraints from small craters, at least in the inner Solar System where we know that many small primary craters are produced.

One approach would be to avoid using craters smaller than the diameter at which the SFD slope b exceeds ~3; this is prudent but not sufficient because small craters can be preferentially erased by many geologic processes, thus hiding the signature of a secondary population. Also, debates continue about whether the primary SFD of asteroidal debris steepens sufficiently at small sizes to produce $b > 3$ for small craters.

Modeling results (Shoemaker 1965, Soderblom et al. 1974, Neukum & Ivanov 1994, McEwen et al. 2005) demonstrate that the crossover diameter (D_c) below which secondaries dominate the statistics must typically be smaller for younger terrains. D_c is controlled by the largest primary crater contributing significant numbers of

secondaries to a terrain, and that largest size is smaller, statistically, over shorter time periods (i.e., younger terrains). There is no guarantee that an especially large impact did not occur sufficiently close to a region of interest in recent times, but such craters can be identified. However, the smaller the crater, the greater the range at which it may have originated if it is a secondary, so using craters that are only tens of meters in diameter for age estimates may be highly problematic. McEwen et al. (2005) recommended the following minimum crater diameters for age constraints on Martian surfaces: 1600 m and 1200 m for the Early and Late Hesperian, respectively; and 840 m, 420 m, and 300 m for the Early, Middle, and Late Amazonian, respectively. It is not advisable at present to use craters below these limits for dating Martian surfaces, and caution is still needed in using craters smaller than a few kilometers in diameter.

On Europa researchers lack the image coverage to globally map secondary fields, and the entire surface may be geologically young, so the best that can be done for now is to define a single threshold diameter such as 1 km for age determination. Note that a 50-million-year surface on Europa may have a much larger crossover diameter than a 50-million-year surface on Mars because the primary production function is flatter on Europa relative to the inner Solar System, whereas the secondary SFD is comparable between inner- and outer–Solar System objects. An even larger crossover diameter is still appropriate for old terrains in the Jupiter system, such as on Ganymede and Callisto.

A possible means to reduce contamination from secondaries would be to map out the known and potential secondary fields of all large young craters. An upper-limit age to the terrain in question must be derived from the absence or paucity of craters larger than a reasonable size such as ~1 km diameter. Researchers could then estimate D_c from the secondary-crater maps and upper-limit age of the terrain. Such maps would also provide relative ages by using secondaries as stratigraphic markers, if their primary-crater origin can be determined.

Small craters offer false promises of statistical robustness and are easily misused for age constraints. The largest errors will always occur when using small craters to date small surface areas. Averaging crater measurements for similar surface units (e.g., debris mantles on Mars) may provide meaningful constraints on age, much as multiple measurements in an ill-behaved experiment can provide meaningful results; one measurement is too noisy, yet multiple measurements provide information. Note, however, that this technique requires that the definition of similar surface units be objective, quantifiable, and repeatable. Researchers using small craters for chronology must be able to present realistic estimates of uncertainties due to imperfect production functions and local contamination by secondaries.

FUTURE STUDIES

A wealth of new high-resolution imaging is being acquired or expected in the next decade, from Cassini (Saturnian moons), Mars Reconnaissance Orbiter and other Mars orbiters, Mercury Messenger, Lunar Reconnaissance Orbiter and other lunar orbiters, and Dawn (large main-belt asteroids). The challenge will be how to analyze

these huge data sets to extract the relevant information about small-crater morphologies and distributions. High-resolution topographic measurements will be especially useful if secondaries can be distinguished from primaries by their depth/diameter ratios or other topographic measurements.

Secondary formation must persist on objects with lower surface gravity, perhaps on objects with escape velocities of only a few hundred meters per second or smaller, as fragments with those velocities form the adjacent secondaries seen on larger bodies. The presence of extensive ejecta blocks on Eros (Thomas et al. 2001, Chapman et al. 2002) demonstrates that even low surface gravity objects such as asteroids retain significant amounts of ejecta; the fragments do not form secondaries because they impact with insufficient velocity. If we assume that 200 m s^{-1} is a minimum velocity for secondary formation, then objects with escape velocities of 300 m s^{-1} will retain some portion of their ejecta that reimpacts with sufficient velocity to form secondaries. That escape velocity corresponds to objects ~450 km diameter for a density of 3 g cm^{-3}, and ~800 km diameter for a density of 1 g cm^{-3}. This suggests that the largest asteroids will exhibit secondary craters, as will mid-sized icy satellites and large Kuiper-belt objects in the outer Solar System. The Cassini images of the Saturnian satellites may provide an opportunity to examine the effect of surface gravity on the relative abundances of secondaries.

It should be possible to measure or place limits on the present-day rate of production of small primary craters by direct observation. Apollo 15–17 panoramic images at 1–2 m resolution cover more than 10% of the Moon. The Lunar Reconnaissance Orbiter, expected to map the Moon in 2009, includes the Lunar Reconnaissance Orbiter Camera (LROC) with ~0.5 m $pixel^{-1}$ imaging (Robinson et al. 2005). The LROC team plans to reimage at least 5% of the Moon's surface previously imaged at 1–2 m resolution to search for new small craters. On the basis of the Neukum production function we should expect ~25 lunar craters ≥10 m diameter to form on the Moon each year, so over 38 years we should find ~47 new primary craters from 10–100 m diameter over 5% of the Moon. If b is less than 3, as we have suggested in this paper, then we may find no new craters larger than 10 m diameter, but new bright spots from the ejecta of even smaller new craters may be seen.

Higher-resolution imaging will enable us to distinguish fresh from degraded craters down to smaller sizes, so we can study how the pristine morphologies vary as a function of target material, inferred impact angle, impact velocity, and interactions with nearby simultaneous craters in a cluster. Perhaps it will eventually be possible to confidently distinguish primaries from secondaries by remote sensing. Then we could determine the primary production function and more confidently use small primary craters for age dating.

SUMMARY POINTS

1. Early observations of lunar crater populations (Shoemaker 1965) noted significant enhancements of small-crater density inside the rays of large primary craters.

2. Recent studies of Europa (Bierhaus et al. 2001, 2005), Mars (McEwen et al. 2005), and the Moon (Dundas & McEwen 2005) show that a single primary impact may generate 10^6–10^8 secondary craters. These secondaries exhibit steep SFDs, extend more than 1000 km from their source crater, and contribute to the spatially random population. Simple scaling to surfaces with many large primary craters demonstrates that the predicted secondary population is comparable to the observed small-crater population.
3. Recent modeling of the excavation process (Head et al. 2002, Artemieva et al. 2004), in part inspired by the presence of Martian and lunar meteorites on Earth, support observations that a single primary impact can generate tens of millions of secondaries.
4. Modeling of asteroid dynamics (Bottke et al. 2005) shows that the expected SFD for near-Earth objects (i.e., the objects that impact the planets of the inner Solar System) is not sufficiently steep to explain the SFDs of small craters on the Moon and Mars.
5. The size-velocity relationship of impact ejecta and the resulting crater SFD (illustrated in this paper) show that secondary craters are expected to have a steeper SFD than primary craters, even if the primary and secondary projectile SFDs are the same. Thus secondaries should dominate below a crossover diameter.
6. The production function for small primary craters on the Moon and Mars has a shallower SFD than commonly used production functions, which must be contaminated by secondaries.
7. The presence of secondaries complicates, but does not invalidate, the use of crater densities to determine relative ages. Certainly craters with diameters larger than a few kilometers on terrains that postdate basin-forming impacts are affected little by secondaries and are valid markers of relative age. We should be able use somewhat smaller craters on young terrains for age dating in the inner Solar System where we know that the production of small primary craters is significant.

ACKNOWLEDGMENTS

The authors thank many colleagues for discussions and communications related to this work, including Natasha Artemieva (Russian Academy of Sciences), Clark Chapman and Bill Bottke (Southwest Research Institute, Boulder), Bill Hartmann and Betty Pierazzo (Planetary Science Institute, Tucson), John Grant (Center for Earth and Planetary Studies, Smithsonian Institution), Matt Golombek (Jet Propulsion Laboratory), Livio Tornabene (University of Tennessee), and Jay Melosh, Elizabeth Turtle, Brandon Preblich, and Colin Dundas (University of Arizona).

LITERATURE CITED

A'Hearn MF, Belton MJS, Delamere WA, Kissel J, Klaasen KP, et al. 2005. Deep impact: excavating comet Tempel 1. *Science* 310:258–64

Anderson JLD, Schultz PH, Heineck JT. 2003. Asymmetry of ejecta flow during oblique impacts using three-dimensional particle image velocimetry. *J. Geophys. Res.* 108(E8):13–1, doi: 10.1029/2003JE002075

Arfstrom J, Hartmann WK. 2005. Martian flow features, moraine-like ridges, and gullies: terrestrial analogs and interrelationships. *Icarus* 174:321–35

Arakawa M, Maeno N, Higa M, Iijima Y, Kato M. 1995. Ejection velocity of ice fragments. *Icarus* 118:341–54

Artemieva NA. 2005. Small primaries versus large secondaries on Mars—numerical approach. *Lunar Planet. Sci.* 36:1589 (Abstr.)

Artemieva NA, Ivanov BA. 2004. Launch of Martian meteorites in oblique impacts. *Icarus* 171:84–101

Arvidson R, Crozaz G, Drozd RJ, Hohenberg CM, Morgan CJ. 1975. Cosmic ray exposure ages of features and events at the Apollo landing sites. *Moon* 13:259–76

Arvidson R, Drozd R, Guinness E, Hohenberg C, Morgan C, et al. 1976. Cosmic ray exposure ages of Apollo 17 samples and the age of Tycho. *Proc. Lunar Sci. Conf.*, *7th*, Houston, 2817–32. New York: Pergamon

Bart GD, Melosh HJ. 2005. Ejected boulders: implications for secondary craters and the age dating of surfaces. *Lunar Planet. Sci.* 36:2022 (Abstr.)

Basilevsky AT, Neukum G, Ivanov BA, Werner SK, Gesselt S, et al. 2005. Morphology and geological structure of the western part of the Olympus Mons volcano on Mars from the analysis of the Mars Express HRSC imagery. *Solar Syst. Res.* 39:85–101

Bierhaus EB. 2004. *Discovery that secondary craters dominate Europa's small crater population*. PhD thesis. Univ. Colo. Boulder. 293 pp.

Bierhaus EB, Chapman CR, Merline WJ. 2005. Secondary craters on Europa and implications for cratered surfaces. *Nature* 437:1125–27

Bierhaus EB, Chapman CR, Merline WJ, Brooks SM, Asphaug E. 2001. Pwyll secondaries and other small craters on Europa. *Icarus* 153:264–76

Bottke WF, Nesvorny D, Durda DD. 2005. Are most small craters primaries or secondaries: insights from asteroid collisional/dynamical evolution models. *Lunar Planet. Sci.* 36:1489 (Abstr.)

Bottke WF, Vokrouhlicky D, Rubicam DP, Nesvorny D. 2006. The Yarkovsky and YORP effects: implications for asteroid dynamics. *Annu. Rev. Earth Planet. Sci.* 34:157–91

Britt DT, Yeomans D, Housen K, Consolmagno G. 2002. Asteroid Density, Porosity, and Structure. In *Asteroids III*, ed. WF Bottke Jr, A Cellino, P Paolicchi, RP Binzel, pp. 485–500. Tucson: Univ. Ariz.

Brown P, Spalding RE, ReVelle DO, Tagliaferri E, Worden SP. 2002. The flux of small near-Earth objects colliding with the Earth. *Nature* 420:294–96

Chapman CR, Haefner RR. 1967. A critique of methods for analysis of the diameter-frequency relation for craters with special application to the moon. *J. Geophys. Res.* 72:549–57

Chapman CR, Merline WJ, Bierhaus EB, Keller J, Brooks S. 1997. Impactor populations on the Galilean satellites. *Bull. Am. Astro. Soc.* 29:984 (Abstr.)
Chapman CR, Merline WJ, Thomas PC, Jospeh J, Cheng AF, Izenberg N. 2002. Impact history of Eros: craters and boulders. *Icarus* 155:104–18
Chapman CR, Veverka J, Belton MJS, Neukum G, Morrison D. 1996. Cratering on Gaspra. *Icarus* 120:231–45
Chappelow JE, Sharpton VL. 2005. Influences of atmospheric variations on Mars' record of small craters. *Icarus* 178:40–55
Culler TS, Becker TA, Muller RA, Renne PR. 2000. Lunar impact history from $^{40}Ar/^{39}Ar$ dating of glass spherules. *Science* 287:1785–88
Doran PT, Clifford SM, Forman SL, Nyquist L, Papanastassiou DA, et al. 2004. Mars chronology: assessing techniques for quantifying surficial processes. *Earth-Sci. Rev.* 67:313–37
Drozd RJ, Hohenberg CM, Morgan CJ, Podosek FA, Wroge ML. 1977. Cosmic ray exposure history at Taurus-Littrow. *Proc. Lunar Sci.* 8:254–56
Dundas C, McEwen AS. 2005. Secondary craters and rays of Tycho. *Geol. Soc. Am. Abstr. Programs* 37:348 (Abstr.)
Fielder G, Fryer RJ, Titulaer C, Herring AK, Wise B. 1972. Lunar crater origin in the maria from analysis of Orbiter photographs. *Philos. Trans. R. Soc.* 271:361–409
Fink J, Gault D, Greeley R. 1984. The effect of viscosity on impact cratering and possible application to the icy satellites of Saturn and Jupiter. *J. Geophys. Res.* 89:417–23
Gault DE, Wedekind JA. 1978. Experimental studies of oblique impact. *Lunar Planet. Sci. Conf. 9 Proc.* 3:3843–75
Gilbert GK. 1893. The Moon's face, a study of the origin of its features. *Bull. Philos. Cos. Wash.* 12:241–92
Grant JA, Arvidson R, Bell JF, Cabrol NA, Carr MH, et al. 2004. Surficial deposits at Gusev crater along Spirit rover traverses. *Science* 305:807–10
Guinness EA, Arvidson RE. 1977. On the constancy of the lunar cratering flux over the past 3.3×10^9 yr. *Proc. Lunar Sci. Conf. 8th* 3:3475–94
Hartmann WK. 1969. Lunar and interplanetary rock fragmentation. *Icarus* 10:201–13
Hartmann WK. 1970. Lunar cratering chronology. *Icarus* 13:209–301
Hartmann WK. 1999. Martian cratering VI: crater count isochrons and evidence for recent volcanism from Mars Global Surveyor. *Meteor. Planet. Sci.* 34:167–77
Hartmann WK. 2005. Martian cratering 8: isochron refinement and the chronology of Mars. *Icarus* 174:294–320
Hartmann WK, Gaskell RW. 1997. Planetary cratering 2: studies of saturation equilibrium. *Meteor. Planet. Sci.* 32:109–21
Hartmann WK, Neukum G. 2001. Cratering chronology and the evolution of Mars. *Space Sci. Rev.* 96:165–94
Hartmann WK, Strom RG, Grieve RAF, Weidenschilling SJ, Diaz J, et al. 1981. Chronology of planetary volcanism by comparative studies of planetary cratering. In *Basaltic Volcanism on the Terrestrial Planets*, pp. 1049–127. New York: Pergamon

Hauber E, van Gasselt S, Ivanov B, Werner S, Head JW, et al. 2005. Discovery of a flank caldera and very young glacial activity at Hecates Tholus, Mars. *Nature* 434:356–61

Head JN, Melosh HJ, Ivanov BA. 2002. Martian meteorite launch: high-speed ejecta from small craters. *Science* 298:1752–56

Herkenhoff KE, Plaut JJ. 2000. Surface ages and resurfacing rates of the polar layered deposits on Mars. *Icarus* 144:243–53

Hiesinger H, Head JW, Wolf U, Jaumann R, Neukum G. 2003. Ages and stratigraphy of mare basalts in Oceanus Procellarum, Mare Nubium, Mare Cognitum, and Mare Insularum. *J. Geophys. Res. Planets* 108(E7):1-1, doi: 10.1029/2002JE001985

Hirase Y, Nakamura AM, Michikama T. 2004. Ejecta size-velocity relation derived from the distribution of the secondary craters of kilometer-sized craters on Mars. *Planet. Space Sci.* 52:1103–8

Holsapple K. 1993. The scaling of impact processes in planetary sciences. *Annu. Rev. Earth Planet. Sci.* 21:333–73

Holsapple K, Giblin I, Housen K, Nakamura A, Ryan E. 2002. Asteroid impacts: laboratory experiments and scaling laws. In *Asteroids III*, ed. WF Bottke, A Cellino, P Paolicchi, RP Binzel, pp. 443–62. Tucson: Univ. Ariz. Press

Horz F, Ostertag R, Rainey DA. 1983. Bunte breccia of the Ries—continuous deposits of large impact craters. *Rev. Geophys. Space Phys.* 21:1667–725

Housen KR, Schmidt RM, Holsapple KA. 1983. Crater ejecta scaling laws: fundamental forms based on dimensional analysis. *J. Geophys. Res.* 88:2485–99

Ivanov BA. 2001. Mars/Moon cratering ratio estimates. *Space Sci. Rev.* 96:87–104

Ivanov BA, Neukum G, Bottke WF, Hartmann WK. 2002. The comparison of size-frequency distributions of impact craters and asteroids and the planetary cratering rate. In *Asteroids III*, ed. WF Bottke, A Cellino, P Paolicchi, RP Binzel, pp.89–101. Tucson: Univ. Ariz. Press

Jedicke R, Larsen J, Spahr T. 2002. Observational selection effects in asteroid surveys and estimates of asteroid population sizes. In *Asteroids II*, ed. WF Bottke Jr, A Cellino, P Paolicchi, RP Benzel, pp. 71–87. Tucson: Univ. Ariz. Press

Kato M, Higa M, Shirai K, Iijima Y, Kiyono T, et al. 2001. Shock pressure attenuation in water ice at a pressure below 1 GPa. *J. Geophys. Res.* 106:17567–78

Kato M, Iijima Y, Arakawa M, Okimura Y, Fujimura A, et al. 1995. Ice-on-ice impact experiments. *Icarus* 113:423–41

Levison HF, Duncan MJ. 1997. From the Kuiper Belt to Jupiter-family comets: the spatial distribution of ecliptic comets. *Icarus* 127:13–32

Levison HF, Duncan MJ, Zahnle K, Holman M, Dones L. 2000. Planetary impact rates from ecliptic comets. *Icarus* 143:415–20

Levy DH. 2000. *Shoemaker: The Man Who Made an Impact*. Princeton, NJ: Princeton Univ. Press. 303 pp.

Malin MC, Edgett KS. 2001. Mars Global Surveyor Mars Orbiter Camera: interplanetary cruise through primary mission. *J. Geophys. Res.* 106:23429–570

Mangold N. 2003. Geomorphic analysis of lobate debris aprons on Mars at Mars Orbiter Camera scale: evidence for ice sublimation initiated by fractures. *J. Geophys. Res.* 108(E4):GDS2-1, doi:10.1029/2002JE001885

Masursky H, Colton GW, El-Baz J, eds. 1978. Apollo over the Moon: a view from orbit. *NASA Spec. Pub.* 362. 255 pp.
McEwen AS, Gaddis LR, Neukum G, Hoffmann H, Pieters C, Head JW. 1993. Galileo observations of post-Imbrium lunar craters during the first Earth-Moon flyby. *J. Geophys. Res.* 98:17207–34
McEwen AS, Preblich BS, Turtle EP, Artemieva NA, Golombek MP, et al. 2005. The rayed crater Zunil and interpretations of small impact craters on Mars. *Icarus* 176:351–81
Mellon MT, Jakosky BM, Kieffer HK, Christensen PR. 2000. High-resolution thermal inertia mapping from the Mars Global Surveyor Thermal Emission Spectrometer. *Icarus* 148:437–55
Melosh HJ. 1984. Impact ejection, spallation, and the origin of meteorites. *Icarus* 59:234–60
Melosh HJ. 1989. *Impact Cratering: A Geologic Process*. New York: Oxford Univ. Press. 253 pp.
Moore HJ, Boyce JM, Han DA. 1980. Small impact craters in the lunar regolith—their morphologies, relative ages, and rates of formation. *Moon Planets* 23:231–52
Morbidelli A, Bottke WF, Froeschle CH, Michel P. 2002. Origin and evolution of near-Earth objects. In *Asteroids III*, ed. WF Bottke, A Cellino, P Paolicchi, RP Binzel, pp. 409–22. Tucson: Univ. Ariz. Press
Morbidelli A, Vokrouhlicky D. 2003. The Yarkovsky-driven origin of near-Earth asteroids. *Icarus* 163:120–34
Murray JB, Muller JP, Neukum G, Werner SC, van Gasselt S, et al. 2005. Evidence from the Mars Express High Resolution Stereo Camera for a frozen sea close to Mars' equator. *Nature* 434:352–56
Nakamura AM, Fujiwara A. 1991. Velocity distribution of fragments formed in a simulated collisional disruption. *Icarus* 92:132–46
Nakamura AM, Fujiwara A, Kadono T. 1994. Velocity of finer fragments from impact. *Planet. Space Sci.* 42:1043–52
Namiki N, Honda C. 2003. Testing hypotheses for the origin of steep slope of lunar size-frequency distribution for small craters. *Earth Planets Space* 55:39–51
Neukum G, Ivanov BA. 1994. Crater size distributions and impact probabilities on Earth from lunar, terrestrial planet, and asteroid cratering data. In *Hazards Due to Comets and Asteroids*, ed. T Gehrels, pp 359–416. Tucson: Univ. Ariz. Press
Neukum G, Ivanov BA, Hartmann WK. 2001. Cratering records in the inner Solar System in relation to the lunar reference system. *Space Sci. Rev.* 96:55–86
Neukum G, Jaumann R, Hoffmann H, Hauber E, Head JW, et al. 2004. Recent and episodic volcanic and glacial activity on Mars revealed by the High Resolution Stereo Camera. *Nature* 432:971–79
Neukum G, Koenig B. 1976. Dating of individual lunar craters. *Lunar Sci. Conf., 7th, Houston* 3:2867–81
Neukum G, Koenig B, Arkani-Hamed J. 1975. A study of lunar impact crater size-distributions. *Moon* 12:201–29
Nyquist LE, Bogard DD, Shih C-Y, Greshake A, Stöffler D, Eugster O. 2001. Ages and geologic histories of Martian meteorites. *Space Sci. Rev.* 96:105–64

This remains the best general reference book on impact cratering.

O'Brien DP, Greenberg R. 2005. The collisional and dynamical evolution of main-belt and NEA size distributions. *Icarus* 178:179–212

Oberbeck VR. 1975. The role of ballistic erosion and sedimentation in lunar stratigraphy. *Rev. Geophys. Space Phys.* 13:337–62

Oberbeck VR, Morrison RH. 1973. On the formation of lunar herringbone pattern. *Proc. Lunar Sci. Conf.* 4:107–23

Onose N, Fujiwara A. 2004. Mass-velocity distributions of fragments in oblique impact cratering on gypsum. *Meteorit. Planet. Sci.* 39:321–31

Pierazzo E, Melosh HJ. 2000. Understanding oblique impacts from experiments, observations, and modeling. *Annu. Rev. Earth Planet. Sci.* 28:141–67

Pike RJ, Wilhelms DE. 1978. Secondary-impact craters on the Moon: topographic form and geologic process. *Lunar Planet. Sci.* 9:907–9 (Abstr.)

Plaut J. 2005. An inventory of impact craters on the Martian south polar layered deposits. *Lunar Planet. Sci.* 36:2319 (Abstr.)

Plescia JB. 2003. Cerberus Fossae, Elysium, Mars: a source for lava and water. *Icarus* 164:79–95

Polanskey CA, Ahrens TJ. 1990. Impact spallation experiments: fracture patterns and spall velocities. *Icarus* 87:140–55

Preblich B, McEwen A, Studer D. 2005. Mapping rays and secondary craters from Zunil, Mars. *Lunar Planet. Sci.* 36:2112 (Abstr.)

Quantin C, Allemand P, Mangold N, Delacourt C. 2004. Ages of Valles Marineris (Mars) landslides and implications for canyon history. *Icarus* 172:555–72

Rabinowitz D, Helin E, Lawrence K, Pravdo S. 2000. A reduced estimate of the number of kilometer-sized near-Earth asteroids. *Nature* 403:165–66

Reiss D, van Gasselt S, Neukum G, Jaumann R. 2004. Absolute dune ages and implications for the time of formation of gullies in Nirgal Vallis, Mars. *J. Geophys. Res.* 109(E6):10.1029/2004JE002251

Roberts WA. 1964. Secondary craters. *Icarus* 3:348–64

Robinson MS, Eliason EM, Hiesinger H, Jolliff BL, McEwen AS, et al. 2005. LROC–Lunar Reconnaissance Orbiter Camera. *Lunar Planet. Sci.* 36:1576 (Abstr.)

Schenk PM, Chapman CR, Zahnle K, Moore JM. 2004. Ages and interiors: the cratering record of the Galilean Satellites. In *Jupiter: The Planet, Satellites and Magnetosphere*, ed. F Bagenal, T Dowling, W McKinnon, pp. 427–56. Cambridge: Cambridge Univ. Press

Schultz PH, Gault DE. 1985. Clustered impacts—experiments and implications. *J. Geophys. Res.* 90:3701–32

Schultz PH, Singer J. 1980. A comparison of secondary craters on the Moon, Mercury, and Mars. *Proc. Lunar Planet. Sci.* 11:2243–59

Shoemaker EM. 1962. Interpretation of lunar craters. In *Physics and Astronomy of the Moon*, ed. Z Kopal, pp. 283–359. New York: Academic

Shoemaker EM. 1965. Preliminary analysis of the fine structure of the lunar surface in *Mare Cognitum*, JPL Tech. Report No. 32–700. In *The Nature of the Lunar Surface*, ed. WN Hess, DH Menzel, JA O'Keefe, pp. 23–77. Baltimore: Johns Hopkins Press

Shoemaker EM, Hackman RJ. 1962. Stratigraphic basis for a lunar time scale. In *The Moon*, ed. Z Kopal, ZK Mikhailov, pp. 289–300. New York: Academic

Eugene M. Shoemaker's landmark papers established how to use impact craters to remotely study planetary surfaces.

Shoemaker EM, Hackman RJ, Eggleton RE. 1962. Interplanetary correlation of geologic time. *Adv. Astronaut. Sci.* 8:70–89

Soderblom LA, Condit CD, West RA, Herman BM, Kreidler TJ. 1974. Martian planetwide crater distributions: implications for geologic history and surface processes. *Icarus* 22:239–63

Strom RG, Croft S, Barlow N. 1992. The Martian impact cratering record. In *Mars*, ed. H Kieffer, B Jakosky, CW Snyder, MS Matthews, pp. 383–423. Tucson: Univ. Ariz. Press

Tanaka KL. 1986. The stratigraphy of Mars. *Lunar Planet. Sci.* 17 and *J. Geophys. Res. Suppl.* 91:E139–58

Thomas PC, Veverka J, Robinson MS, Murchie S. 2001. Shoemaker crater as the source of most ejecta blocks on the asteroid 433 Eros. *Nature* 413:394–96

Tornabene LL, McSween HY, Moersch JE, Piatek JL, Milam KA, Christensen PR. 2005. Recognition of rayed craters on Mars in THEMIS thermal infrared imagery: implications for Martian meteorite source regions. *Lunar Planet. Sci.* 36:1970 (Abstr.)

Vickery AM. 1986. Size-velocity distribution of large ejecta fragments. *Icarus* 67:224–36

Vickery AM. 1987. Variation in ejecta size with ejection velocity. *Geophys. Res. Lett.* 14:726–29

Warren PH, Taylor GJ, Keil K. 1983. Regolith breccia Allan Hills A81005: evidence of lunar origin and petrography of pristine and nonpristine clasts. *Geophys. Res. Lett.* 10:779–82

Werner SC, Harris AW, Neukum G, Ivanov BA. 2002. The near-Earth asteroid size-frequency distribution: a snapshot of the lunar impactor size-frequency distribution. *Icarus* 156:287–90

Werner SC, van Gesselt S, Neukum G. 2003. Continual geological activity in Athabasca Valles, Mars. *J. Geophys. Res.* 108:ROV 22-1, doi: 10.1029/2002JE002020

Wilhelms DE. 1987. The geologic history of the moon. *U.S. Geol. Surv. Prof. Pap. 1348*. 302 pp.

Wilhelms DE, Oberbeck VR, Aggarwal HR. 1978. Size-frequency distributions of primary and secondary lunar impact craters. *Proc. Lunar Planet. Sci.* 9:3735–62

Yamamoto S. 2002. Measurement of impact ejecta from regolith targets in oblique impacts. *Icarus* 158:87–97

Yamamoto S, Kadono T, Sugita S, Matsui T. 2005. Velocity distributions of high-velocity ejecta from regolith targets. *Icarus* 178:264–73

Zahnle KH, Dones L, Levison H. 1998. Cratering rates on the Galilean satellites. *Icarus* 136:202–22

Zahnle KH, Schenk P, Levison H, Dones L. 2003. Cratering rates in the outer Solar System. *Icarus* 163:263–89

Annual Review of Earth and Planetary Sciences

Volume 34, 2006

Contents